Lamination of Transparent Conductive Adhesives for Tandem Solar Cell Applications

Talysa R. Klein[1], Michelle S. Young[1], Adele C. Tamboli[1] and Emily L. Warren[1]

[1] National Renewable Energy Laboratory (NREL), 15013 Denver West Parkway, Golden, CO 80401, United States of America

E-mail: Talysa.Klein@nrel.gov

Received xxxxxx
Accepted for publication xxxxxx
Published xxxxxx

Abstract

A transparent conductive adhesive (TCA) interlayer for mechanically stacked multijunction solar cells provides adhesive strength and electrical connection between sub-cells when stacked. The fabrication of TCA sheets from an ethyl-vinyl acetate (EVA) matrix and silver coated compliant conductive microspheres, similar to industry-standard EVA encapsulant sheets, compatible with a standard lamination process was developed. Blade coating TCA sheets using 3D printed blades and testing of vertical conduction through the interlayer with a TCA conductivity jig allowed for reproducible measurements and low-cost fabrication. The supplemental information provides design files to enable other researchers to produce their own blades and testing jigs. We identified 0.5 mm as an optimal blade height for producing lab-scale TCA sheets and 120 °C at 3 psi for 10 mins as the optimal vacuum lamination process to minimize resistance and possible damage to samples. For TCA sheets with coverages between 0.75% and 9%, the series resistance was approximately 0.2 Ω-cm^2 which should result in minimal losses for 1-sun photovoltaic applications.

Keywords: TCA, transparent conductor, conductive adhesives, lamination, tandem, solar cell

1. Introduction

Hybrid tandem solar cells are an emerging research area that enables efficiencies that exceed the detailed balance limit of a single material by combining strategic band-gaps of materials to maximize the amount of solar energy converted/absorbed by a given area [1]. There are a variety of growth/integration processes that can be used to create hybrid tandems. Among these is the process of mechanical stacking, which retains the highest efficiencies of each sub-cell by combining independently optimized cells into a tandem structure [2]. Tandem solar cells can have several different terminal configurations: two-terminal (2T), three-terminal (3T), and four-terminal (4T). 2T tandems are electrically connected through a middle interlayer, often a tunnel junction. Similar to 2T tandems, 3T tandems are also electrically interconnected through a middle layer, with the addition of a third terminal, usually from the bottom cell. In 4T tandems cells, the top and bottom sub-cells are electrically isolated from each other and current must be transported laterally between the cells [3]. Within the context of tandems that are mechanically stacked, the interlayer plays a key role in maintaining adhesion between the sub-cells, and must be sufficiently transparent as to not affect the bottom cells efficiencies [4]. For the case of 2T and 3T tandems, the interlayer must also provide a vertical electrical connection, but lateral conductivity is not required [5].

Various approaches to making an interlayer have been experimented with for mechanically stacked tandem cells. Wafer bonding two cells of different lattices is energy intensive and can cause cracking in one of both of the sub-cells as a result of differential thermal expansion coefficients.

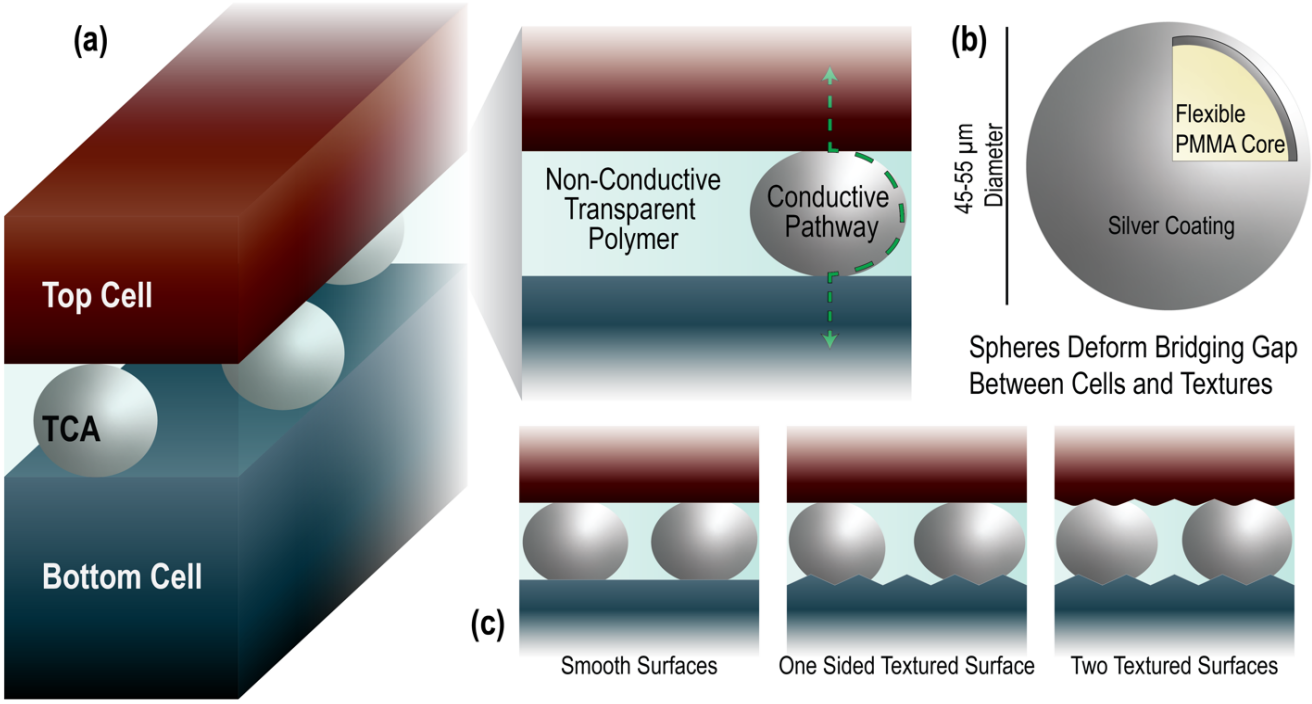

Figure 1: (a) Transparent conductive adhesive (TCA) shown within a tandem solar cell stack, as a single layer of conductive microspheres (45-55µm in diameter) held in place with a transparent non-conductive polymer. (b) The compliant microspheres are a flexible poly(methyl methacrylate) (PMMA) core with a silver coating (c) allowing the spheres to electrically connect smooth and textured surfaces with micron sized surface features.

Nanoparticle and nanowire interlayers can be transparent and conductive, but due to the size of the conductive structures the layers are not able to span textured/uneven non-polished surfaces efficiently, requiring thicker interlayers [6]. Direct metal interconnection requires full grids on the backside of the top cell and topside of bottom cell; this leads to a highly conductive interlayer, precise alignment is required, and the resulting shading losses are not insignificant [7]. Additional methods such as nanoimprint and photolithography have been used to make microstructures that are effective to fabricate on a lab-scale but can get costly when moving to large-scale operations.

The approach described here utilizes a transparent conductive adhesive (TCA) fabricated from a transparent polymer adhesive matrix and compliant conductive microspheres. This TCA provides the necessary properties for making vertical electrical connections for mechanically stacked tandems (Fig 1) [8]. In Figure 1a, the TCA is depicted between a generic top and bottom cell, a monolayer of spheres is formed between the surfaces, with the compliant spheres acting as a spacer. Additionally, the compliancy of the spheres from the PMMA core (Fig 1b) allows the spheres to deform under pressure, increasing the contact area between the spheres and the surface regardless of texture (Fig 1c). We have developed a method for fabrication of TCA "sheets," similar to industry-standard EVA encapsulant sheets, compatible with a standard lamination process to join sub-cells together.

TCAs have been used in the fabrication of several tandem devices. A 27.3% efficient 3T tandem consisting of GaInP and Si (GaInP/s/nuIBC) was reported by Schnabel et al [5], using a TCA with 3% coverage of conductive microspheres in an epoxy matrix deposited as a liquid and processed by hot pressing. Similarly, VanSant et al. fabricated superstrate configuration 3T III-V//Si devices (both GaAs/s/nuIBC and GaInP/s/nuIBC) with efficiencies of 22.5% [9] using pre-cast TCA sheets in an ethyl-vinyl acetate (EVA) matrix and 5% loading of conductive particles in TCA and a vacuum lamination process, as described here. Other efforts have used the TCA to mechanically stack 2T perovskite//Si tandems with an interlayer at 0.5wt% and resistances around 0.05 Ω-cm^2, and an efficiency of 19.4% [10].

Through-plane conduction, or vertical conduction through an interlayer is essential to how the TCA functions, connecting the two surfaces together both electrically and mechanically. The most common measurement of resistances is the traditional TLM approach [11]. However, this approach is typically performed on a surface to calculate the contact resistances and the material sheet resistance, requiring an open surface to probe various pads at specific spacing. With the TCA reliant on the compressive forces between the substrates, as shown in Figure 1, traditional

TLM measurement wouldn't be possible in the current configuration. Here, we describe the development of methods for repeatable measurements of interlayer resistance through the plane while sustaining the adhesive forces of the polymer matrix needed to maintain electrical contact between the surfaces.

The fabrication of commercial solar modules uses encapsulant sheets in vacuum lamination processes to protect and adhere the cells within an array [12]. Commercially available transparent thermoplastic encapsulant sheets such as EVA, TPU, PVA, etc. are used for commercial solar module fabrication. In order to make the TCA easily adapted to industry, we have processed the TCA into sheets similar to commercially available encapsulants. While the sheets can be used in a hot press as explored in previous work [8], a vacuum lamination process lowers the probability of bubbles remaining in the interlayer during processing, which can cause optical losses and lower device reliability (Fig 2). Compatibility of the solar cell materials with the encapsulants/TCA is to be considered on a case-by-case basis, i.e. solution processed perovskite tandems may degrade if there is residual solvent within the TCA [13]. In addition, the processing requirements of the materials for temperatures, pressure, and time will need to be optimized for each tandem stack. General guidelines around current commercially available transparent thermoplastic encapsulant sheets, such as EVA, use processing temperatures and time of 140-160°C and 8-20 min, respectively, similar to our optimized conditions[14].

In this work, we demonstrate a scalable fabrication approach to make TCA sheets for vacuum lamination processes and study the conductivity for the interlayer for various methods of manufacturing and laminating the sheets. We optimize sphere loading and processing conditions to understand their effects on the conductivity of the interlayer. In addition, we discuss testing procedures for through plane conduction measurements.

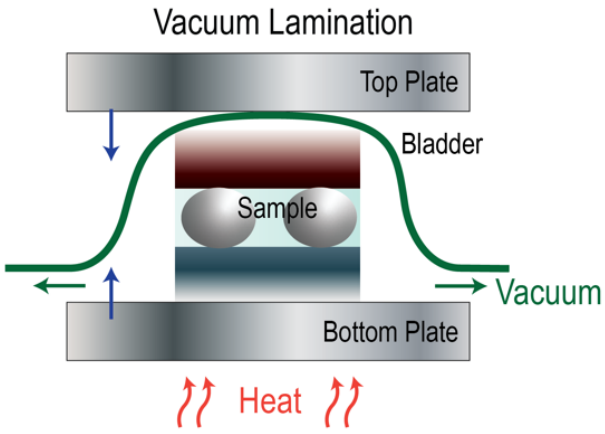

Figure 2: The processing of a tandem solar cell with TCA interlayer sheets using a vacuum lamination process. While the top and bottom plate apply pressure, the sample is also subjected to a vacuum that prevents bubbles from being trapped in the sample.

2. Methods

TCAs were prepared by mixing conductive microspheres with a thermoplastic polymer matrix. Figure 3 shows the process used in this work to create a dispersion of microspheres in EVA. In prior work, the TCA was cast from a liquid and hot pressed, but this process limits the ability to precisely align the top and bottom sub-cells [8]. We developed a process to fabricate sheets of TCA which enables improved alignment between samples and adoption

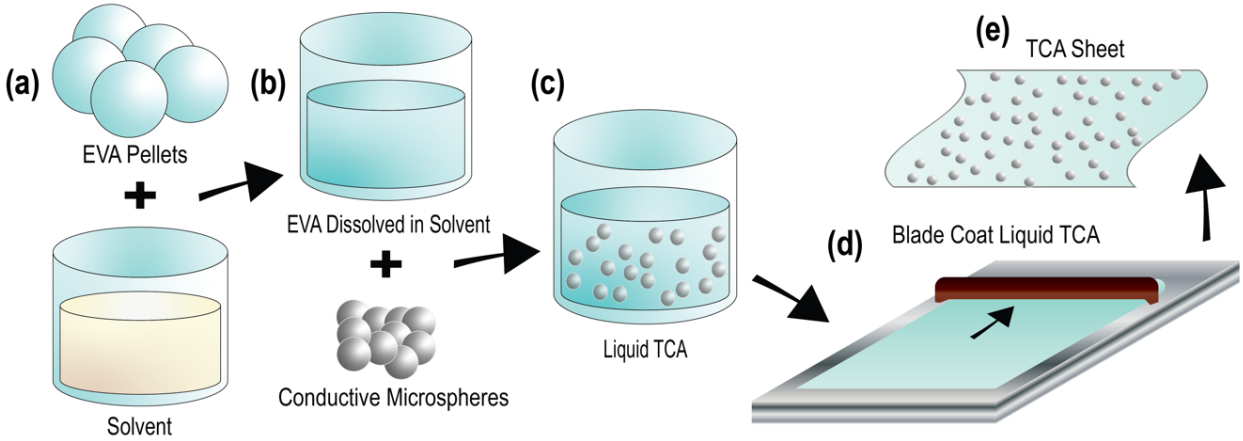

Figure 3: Fabrication of TCA sheets: (a) EVA pellets dissolved in a solvent (such as toluene, chloroform, etc.), (b) the conductive microspheres are then added to the EVA mixture, this creates (c) a liquid TCA. (d) The liquid TCA is then blade coated on PTFE-coated fiberglass sheets, heated to remove residual solvent, then cooled so that the PTFE-coated fiberglass sheet can be removed leaving (e) the TCA sheet.

of a lamination process for thermal curing. Replicating the existing EVA sheets currently used for encapsulation processes allowed for the TCA to utilize the same equipment, such as a vacuum laminator [8]. This process resulted in precise alignment, fewer processing steps, and increased conductivity of the interlayer. For this work an EVA based TCA was used to create the TCA sheets, however other thermoplastics can be used in substitution for the same process depicted in Figure 3.

EVA pellets (ELVAX1000) were dissolved in Toluene in a 1:5 v/v, as described in previous publications (Fig 3a) [8]. Silver coated PMMA conductive spheres (Cospheric PMPMS-AG-1.53 45-53 µm) were added to this in the desired weight to ensure the correct percent coverage of sheets in the laminated film (Fig 3b). After mixing on a hot plate with a magnetic stir bar the mix was referred to as the liquid TCA (Fig 3c). This mixture had a two-week shelf-life before the spheres agglomerate. These agglomerations do not break apart in hot pressing or lamination thus causing an uneven film thickness and conduction over the film.

Blade coating the liquid TCA into sheets distributes the microspheres evenly throughout the thin film and prevents agglomeration during storage. Blade coating blades are available from a variety of retailers; however, a low-cost blade can be easily 3D printed as long as the material is compatible with the solvent. We used toluene; thus, Ultem (Stratasys Ultem 9085) was used as a filament without a surface coating. 3D printed blades at blade heights of 0.25, 0.5, 0.75, and 1 mm were designed and printed using a Stratasys 3D printer (blade .stl file available for download in SI). The verification of blade heights was completed using feeler gauges on the final 3D parts. The liquid TCA was blade coated by hand on PTFE-coated fiberglass sheets (Fig 3d). The film was cured on a 100 ºC hot plate for 10 min, cooled for 5 min, then peeled from the PTFE-coated fiberglass sheet in a single motion avoiding deformation and tearing of the thin TCA sheet (Fig 3e). The TCA sheets can be stored in a dry, particle free environment for up to one month.

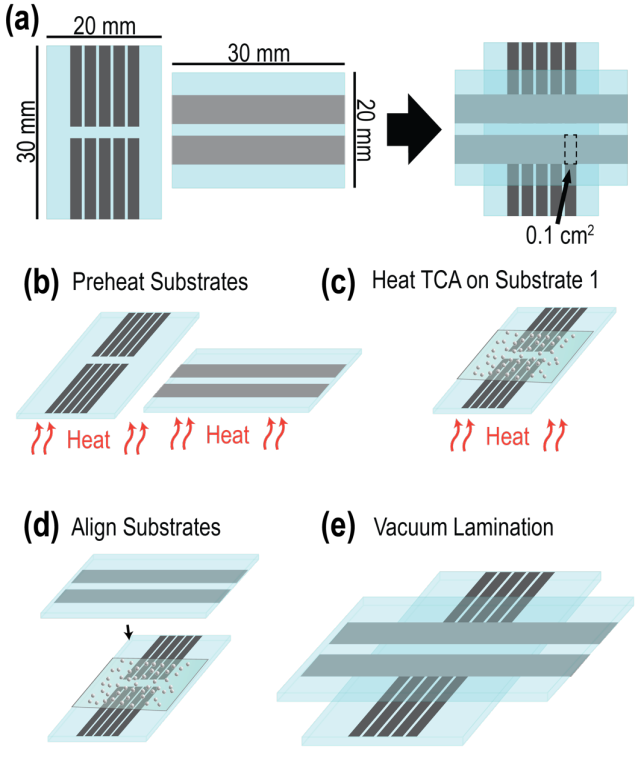

Figure 4: (a) Design of TCA test structures for measuring vertical conduction of the TCA, utilizing the TCA sheet lamination process. (b) Both substrates are first preheated, (c) a cut to size piece of TCA sheet is added to substrate 1 while still being heated to soften the TCA. (d) Then the substrates are aligned and tacked before (e) finishing in the vacuum laminator.

The sample design used for testing electrical conductivity of the TCA when laminated between two surfaces is shown in Figure 4a, where there are 10 pixels of area 0.1 cm^2 in each test structure. Substrates were 1 mm glass with a 20 nm IZO adhesion layer and 150 nm of silver. These substrates were fully coated with metal, laser scribed to define the contact pads, then cut to the desired pattern size. Using a multimeter each pad was verified to be electrically isolated before lamination. With this approach a variety of areas were scribed and tested to ensure the accuracy of the measurements across a variety of testing areas. The overlapping areas for series resistance calculations were determined from the finished laminated test structures by imaging using an optical microscope.

The TCA test structures were processed with varied heat and pressure in a vacuum laminator. The substrates were pre-heated at 100 °C for 10-30 s on a hotplate (Fig 4a). The TCA sheet was cut to the size of the overlapping section of the samples and placed on the first substrate (Fig 4b). The TCA sheet was allowed to soften on the hotplate (5 s). After removing from heat, the second substrate was positioned over the first substrate and pressed together lightly by hand, bonding them together (Fig 4c). This “tacks” the two substrates together temporarily, allowing for precise alignment before finishing the processing in the vacuum laminator (Fig 4d). The vacuum laminator (Bent River SPL2828 PIN) was run with custom recipes varying the temperature (100°C to 130°C in 10°C increments), pressure (3 – 10 psi), and time (5-20 min) to bond the substrates together.

Each film was characterized by the coverage of microspheres. Images of the TCA test structures were taken in 3-4 locations along each sample. The images were processed through binary filters calculating the average pixel coverage of spheres at various magnifications to calculate the areal coverage of the spheres (additional information is SI). This areal coverage directly correlates to the optical

transparency of the TCA since the transparent polymer matrix is optically clear at visible wavelengths and the microspheres are opaque [8].

To enable highly repeatable measurements for a wide range of coverages, processing conditions, and substrate materials, testing jigs were designed and fabricated to measure the electrical properties of the TCA. Using 3D printing, laser-cut acrylic, and spring-loaded contacting pins, each metal pad was contacted with 2 pins enable 4-point conductivity measurements of the TCA. The design progressed through multiple iterations that are discussed and available for download in supplementary information. Figure 5 shows the final version of the testing jig, cut from 5 mm thick clear acrylic with gold-plated spring-loaded pins. Connected to the undersides of the top substrate and the topside of the bottom substrate (Fig 5b), each pad is connected to 2 pins for a 4-point measurement on to the sample, eliminating the contact resistance of pin. In addition, the shape, size, and position of the pins resulted in self-alignment of the testing structures within the jig. Each pin is soldered to external wires for convenient connections. Using two test leads connected to a current source and two test leads connected to a multimeter, the voltage of each pixel was recorded for a given current supplied (values between 1μA-10mA). From this the resistance of the pixel over a given area was calculated as series resistance in Ω-cm^2, calculated from:

$$Series\ Resistance = \frac{Voltage}{Current}(Area_{Pixel})$$

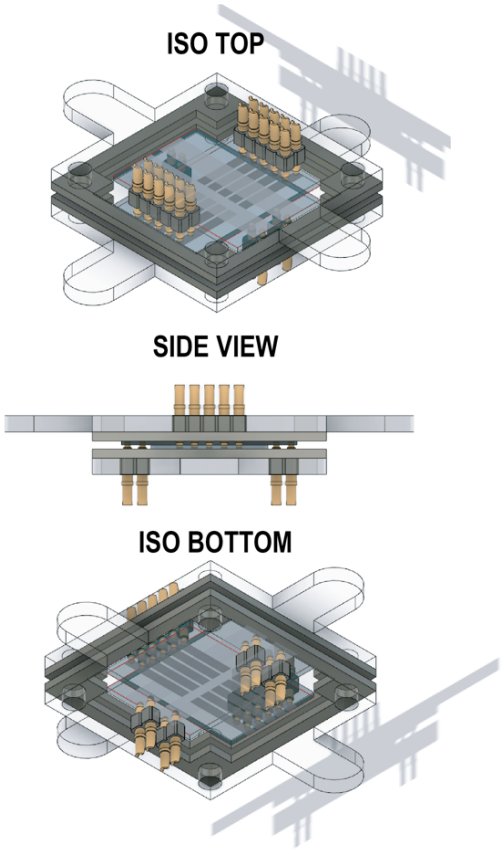

Figure 5: A TCA testing jig shown from different viewpoints was laser cut from clear acrylic with 28 connecting pins that contacted the undersides of the TCA testing structures for taking 4-point resistance measurements of the TCA.

3. Results

The height of the blade used during the blade coating process has large effects in the final conductivity of the interlayer since it sets the thickness of the sheet and adjusts the ratio of spheres to EVA in the sheet (i.e. the thicker the sheet, the more EVA is present around the spheres). If the blade height is too high the resulting film is too thick. This will result in the TCA not compressing enough during processing and will not make connection between the substrates. However, at blade heights under 0.5 mm the resulting series resistance is constant (within error). This finding supports the hypothesis that the spheres act as a spacer between the surfaces resulting in the same final interlayer thickness, equal to the sphere diameter (Supplemental Figure S7). Therefore, conductivity for the same percent coverages of spheres is the same. It is also of note that TCA sheets made with blade heights < 0.25 mm can easily tear when being removed from the PTFE-coated fiberglass sheet, thus a blade height of 0.5 mm was chosen as the optimal height for casting TCA sheets.

In Table 1 the series resistance of the TCA is shown after lamination at various pressures and temperatures. Temperature does not have a large influence on the series resistance, as all the series resistance values for varying temperature were within the error of the testing. However, samples laminated at 100 °C could be easily mechanically separated after lamination. Samples processed at 120 °C produced low-resistance connection with the highest yields, 25%, 25%, and 45% for pressures of 3 psi, 5 psi, and 10 psi, respectively, with the decrease in yield due to cracking or insufficient TCA sheet between the overlapping substrates (see supplemental information for modes of failure discussion). As expected, when samples were laminated at very high pressure, they were more likely to crack during processing due to the mismatched areas needed to contact both sides, as shown by half of the samples processed at 10 psi being cracked. The glass substrates are more robust than some solar cells components but can crack more easily because of their mismatched areas. Cracked cells at the final step in processing when making a tandem device is costly and can be prevented by using processing conditions that don't pose a risk of damaging the samples; thus, we chose the lowest pressure that consistently resulted in adhesion and low resistance. The optimized conditions of 3 psi for

Table 1: Series resistance per square centimeter for 5% coverage of microspheres within the TCA at varied temperature and pressures during the lamination process (laminated for 10 minutes each). All resistances were measured vertically through the interlayer of TCA with the yield of samples and notes (in red) on if the samples were damaged during the lamination process. Yield was calculated from 20 measurements. Low yield was primarily due to cracking caused by pressure applied to unsupported glass outside of the overlap area.

	100°C	**110°C**	**120°C**	**130°C**
3 PSI	0.369±1 Ω-cm² (5% yield) TCA Delamination	1.24±1 Ω-cm² (5% yield) Disconnected Pixels	0.266±0.120 Ω-cm² (25% yield) Disconnected Pixels	0.232± 0.102 Ω-cm² (10% yield) Sample Cracking
5 PSI	0.138±0.026 Ω-cm² (10% yield) Disconnected Pixels	0.169± 0.0327Ω-cm² (20% yield) Sample Cracking	0.197± 0.039Ω-cm² (25% yield) Sample Cracking	0.646± 0.617Ω-cm² (25% yield) Sample Cracking
10 PSI	0.158± 0.048Ω-cm² (45% yield) Sample Cracking	0.216± 0.033Ω-cm² (30% yield) Sample Cracking	0.158± 0.021Ω-cm² (45% yield) Sample Cracking	0.383± 0.336Ω-cm² (10% yield) Sample Cracking

pressure and 120 °C temperature were chosen to minimize cell losses due to cracking and ensure reliability of conduction and processing. These conditions were used to characterize various area coverage of spheres.

TCA sheets can be made with different concentrations of conductive microspheres, and it has previously been demonstrated that the coverage is directly proportional to the transparency of the interlayer [8]. Thus, the series resistance vertically through the interlayer normalized to area is plotted vs. area coverage of microspheres in Figure 6. TCA sheets between 0.75% and 9% area coverage were laminated at 120 °C and 3 psi for 10 minutes. The series resistance remains around 0.2 Ω-cm² for these coverages and processing conditions. Coverages less than 2% had greater variability in the series resistance, increasing the uncertainty of the values.

The desirable area coverage range for tandem solar cells is less than 5% coverage, as the transparency and electrical conduction in that range are sufficient to minimize losses in the bottom cell due to absorption and parasitic resistance losses of the system. TCA sheets between 2% and 5% area coverage laminated at 120°C and 3 psi for 10 minutes is recommended to laminate sub-cells for tandem applications.

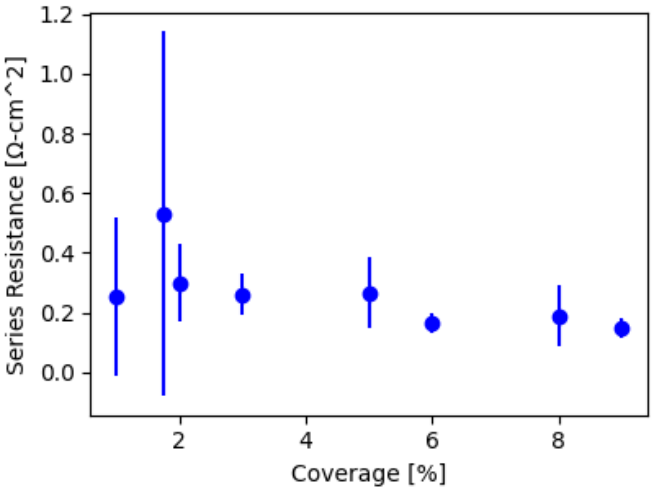

Figure 6: Series resistance per square centimeter vs coverage of microspheres within the TCA. All resistances measured vertically through the interlayer of TCA (laminated at 120°C, 3 psi, and 10 minutes).

4. Conclusions

In this work, we investigate the fabrication of TCA sheets for the use in mechanically stacked multijunction solar cells. The TCA sheets are similar to industry-standard EVA encapsulant sheets, compatible with a standard lamination process to join sub-cells together. We show that blade coating fabrication is a scalable approach to making TCA sheets. The supplemental information provides design files to enable other researchers to produce their own blades and testing jigs. We identified 0.5 mm as an optimal blade height to produce lab-scale TCA sheets with various coverages of spheres. An optimized vacuum lamination process of 120 °C, 3 psi, 10 min was shown to minimize resistance and damage to samples for TCA films with coverages between 0.75% and 9%. The series resistance of these samples coverages was approximately 0.2 Ω-cm² which should result in minimal losses for 1-sun photovoltaic applications. Using TCA sheets of 2% to 5% coverages are recommended for tandem applications to retain transparency and electrical conduction between the sub-cells.

Acknowledgements

The authors thank, Maikel van Hest, Michael Kempe, Kaitlyn VanSant, William McMahon, Pauls Strandins, and John Geisz for helpful discussions. This work was supported by the U.S. Department of Energy under Contract No. DE-AC36-08GO28308 with Alliance for Sustainable Energy, LLC, the Manager and Operator of the National Renewable

Energy Laboratory. Funding provided by the Department of Energy Office of Energy Efficiency and Renewable Energy Solar Energy Technologies Office under contract SETP DE-EE00034911. The views expressed in the article do not necessarily represent the views of the DOE or the U.S. Government. The U.S. Government retains and the publisher, by accepting the article for publication, acknowledges that the U.S. Government retains a nonexclusive, paid-up, irrevocable, worldwide license to publish or reproduce the published form of this work, or allow others to do so, for U.S. Government purposes.

References

[1] M. A. Green, E. D. Dunlop, J. Hohl-Ebinger, M. Yoshita, N. Kopidakis, and A. W. Y. Ho-Baillie, "Solar cell efficiency tables (Version 55)," *Prog. Photovolt. Res. Appl.*, vol. 28, no. 1, pp. 3–15, 2020, doi: 10.1002/pip.3228.

[2] Y. Mols, L. Zhao, G. Flamand, M. Meuris, and J. Poortmans, "Annual energy yield: A comparison between various monolithic and mechanically stacked multijunction solar cells," in *2012 38th IEEE Photovoltaic Specialists Conference*, Jun. 2012, pp. 002092–002095, doi: 10.1109/PVSC.2012.6318010.

[3] E. L. Warren *et al.*, "A Taxonomy for Three-Terminal Tandem Solar Cells," *ACS Energy Lett.*, vol. 5, no. 4, pp. 1233–1242, Apr. 2020, doi: 10.1021/acsenergylett.0c00068.

[4] I. Mathews, D. O'Mahony, K. Thomas, E. Pelucchi, B. Corbett, and A. P. Morrison, "Adhesive bonding for mechanically stacked solar cells," *Prog. Photovolt. Res. Appl.*, vol. 23, no. 9, pp. 1080–1090, 2015, doi: https://doi.org/10.1002/pip.2517.

[5] M. Schnabel *et al.*, "Three-terminal III–V/Si tandem solar cells enabled by a transparent conductive adhesive," *Sustain. Energy Fuels*, 2020, doi: 10.1039/C9SE00893D.

[6] S. Yoshidomi, J. Furukawa, M. Hasumi, and T. Sameshima, "Mechanical Stacking Multi Junction Solar Cells Using Transparent Conductive Adhesive," *Energy Procedia*, vol. 60, pp. 116–122, 2014, doi: 10.1016/j.egypro.2014.12.352.

[7] M. Yamaguchi, K.-H. Lee, K. Araki, and N. Kojima, "A review of recent progress in heterogeneous silicon tandem solar cells," *J. Phys. Appl. Phys.*, vol. 51, no. 13, p. 133002, Apr. 2018, doi: 10.1088/1361-6463/aaaf08.

[8] T. R. Klein *et al.*, "Transparent Conductive Adhesives for Tandem Solar Cells Using Polymer–Particle Composites," *ACS Appl. Mater. Interfaces*, vol. 10, no. 9, pp. 8086–8091, Mar. 2018, doi: 10.1021/acsami.8b00175.

[9] VanSant K T, Warren E L, Geisz J F, Klein T R and Tamboli A C 2021 Design flexibility of 3-terminal tandems: a performance comparison between GaInP//Si and GaAs//Si Prep

[10] I. Y. Choi *et al.*, "Two-terminal mechanical perovskite/silicon tandem solar cells with transparent conductive adhesives," *Nano Energy*, vol. 65, p. 104044, Nov. 2019, doi: 10.1016/j.nanoen.2019.104044.

[11] S. Guo, G. Gregory, A. M. Gabor, W. V. Schoenfeld, and K. O. Davis, "Detailed investigation of TLM contact resistance measurements on crystalline silicon solar cells," *Sol. Energy*, vol. 151, pp. 163–172, Jul. 2017, doi: 10.1016/j.solener.2017.05.015.

[12] A. W. Czanderna and F. J. Pern, "Encapsulation of PV modules using ethylene vinyl acetate copolymer as a pottant: A critical review," *Sol. Energy Mater. Sol. Cells*, vol. 43, no. 2, pp. 101–181, Sep. 1996, doi: 10.1016/0927-0248(95)00150-6.

[13] T. Moot *et al.*, "Choose Your Own Adventure: Fabrication of Monolithic All-Perovskite Tandem Photovoltaics," *Adv. Mater.*, p. 2003312, Nov. 2020, doi: 10.1002/adma.202003312.

[14] C. Wiesmeier, I. Haedrich, K.-A. Weiss, and I. Duerr, "Overview of PV module encapsulation materials," *Photovolt. Int.*, vol. 19, pp. 85–92, Jan. 2013.